JOURNAL OF CATALYSIS 106, 176–187 (1987)

Activated Chemisorption of Hydrogen on Supported Ruthenium

II. Effects of Crystallite Size and Adsorbed Chlorine on Accurate Surface Area Measurements

K. LU AND B. J. TATARCHUK[1]

Department of Chemical Engineering, Auburn University, Auburn, Alabama 36849

Received August 12, 1986; revised February 25, 1987

A crystallite size effect has been observed during the activated adsorption of hydrogen on supported ruthenium catalysts. This effect does not occur in the absence of adsorbed chlorine and is increasingly more pronounced as metal dispersion is increased. Activation energies for adsorption, at constant hydrogen coverage, may be as high as 16 kcal/mole and have been measured utilizing (i) Al_2O_3 and SiO_2 support materials, (ii) crystallites which range in size from 2.6 to 22.0 nm, and (iii) surface chlorine coverages which vary from 0.01 to 0.35 of the number of surface ruthenium atoms. Results of these studies suggest that preferential adsorption of chlorine atoms at high coordination sites reduces electron density at adjacent low coordination sites, thereby increasing the activation energy barrier for electron donation to, and dissociative chemisorption of, incoming hydrogen molecules. While this effect may be viewed as primarily electronic in origin, a structure-sensitive (i.e., crystallite size-dependent) mechanism has been proposed to account for the observed adsorption behavior based on the number of high coordination-chlorine adsorption sites in close proximity to low coordination-hydrogen adsorption sites. Activated adsorption sites, attributed to the above-noted mechanism, can be responsible for a greater than two-fold underestimation of the number of surface ruthenium atoms measured by irreversible hydrogen adsorption at 298 K. Significant differences in adsorption behavior between silica- and alumina-supported crystallites of equal dispersion also suggest that deliberate addition of chlorine adatoms may provide a sensitive probe for discriminating differences in crystallite shape and surface texture. © 1987 Academic Press, Inc.

INTRODUCTION

Differences in the catalytic and chemisorptive behavior of supported metal crystallites of various size has been an area of major research interest in the past. General explanations for such effects can be viewed with respect to two distinctly different perspectives. From a *geometric* standpoint, the surface morphologies of small crystallites are expected to differ from those of larger crystallites resulting in different proportions of coordinatively unsaturated edge and corner sites. These coordinatively unsaturated sites may have different chemical/physical properties compared to surface atoms of higher coordination number. From an *electronic* standpoint, small crystallites are also more likely to be influenced by metal–support interactions and may not provide bulk electronic band structures if they are extremely small.

Previous efforts have demonstrated that the intrinsic reaction and adsorption properties of supported ruthenium catalysts change with crystallite size (*1–5*). For example, by studying cyclohexane conversion on supported ruthenium catalysts, Lam and Sinfelt (*1*) found that the ratio of dehydrogenation to hydrogenolysis events increased by more than a factor of 10 with decreasing crystallite size. Dalla Betta (*2*) and Yang and Goodwin (*3*) found that the CO/H uptake ratio as well as the carbon–oxygen stretching frequency differed with

[1] Author to whom correspondence should be addressed.

0021-9517/87 $3.00
Copyright © 1987 by Academic Press, Inc.
All rights of reproduction in any form reserved.

crystallite size. Taylor (*4*) investigated oxygen chemisorption and oxygen–hydrogen titration over supported ruthenium catalysts and claimed that it was inappropriate to use these methods for crystallites less than 4.0 nm since significant changes in adsorption stoichiometry occurred. More recently, Sayari *et al.* (*5*) observed a size-dependent trend in reversible adsorption isotherms measured at 298 K.

In Part I of this study (*6*), the effects of chlorine additives on the chemisorptive properties of supported ruthenium catalysts were investigated. It was observed that hydrogen chemisorption over supported ruthenium crystallites became activated in the presence of chlorine adatoms apparently due to an electronic perturbation of the metal by chlorine. What is still unclear, however, is the crystallite size dependence of this chlorine-induced behavior. In this study, alumina- and silica-supported ruthenium catalysts, with a range of average crystallite diameters between 2.6 and 22.0 nm, have been studied to provide a more comprehensive understanding of the relative influence of chlorine additives versus crystallite size. This information is crucial in understanding the site requirements for chlorine adsorption and its subsequent impact on the kinetic energy barrier encountered during hydrogen adsorption.

EXPERIMENTAL

Materials. Catalyst supports used include a Harshaw Al-3945 alumina powder, 234 m^2/g, and a Davison grade 56 silica powder, 300 m^2/g. The chlorine content in the bulk of these supports was 45 ± 1 and 22 ± 1 ppm, respectively, as determined by bulk analyses (Galbraith). Hydrogen and helium used in this study were Linde prepurified grade (99.99% purity) and were further purified by passage through a Deoxo unit at 298 K, a copper turning trap at 500 K, and a 5X molecular sieve trap at 77 K. Carbon monoxide (99.8%–Air Products) was treated by passage over a Deoxo unit at 298 K, a 5X molecular sieve trap at 500 K, and finally another bed of 5X molecular sieves at 196 K. Ultrapure oxygen (99.99%) from a local vendor was purified with 5X molecular sieves at 196 K.

Catalysts. Both commercial and laboratory prepared catalysts were used in this study. The commercial catalyst used was a 5% Ru/Al_2O_3 catalyst from Engelhard (BET = 120 m^2/g) while laboratory catalysts were prepared by incipient wetness impregnation of $RuCl_3$ and vapor decomposition/deposition of $Ru_3(CO)_{12}$. These preparation procedures have been described earlier (*6*). All catalysts employed in this study were denoted by a prefix referring to their sources. An "I" represents catalysts prepared from incipient wetness impregnation using $RuCl_3$; a "V" represents catalysts prepared by vapor decomposition/deposition using $Ru_3(CO)_{12}$; and a "C" represents catalysts obtained from the commercial vendor.

Catalyst pretreatment, reduction, and adsorption. Volumetric hydrogen adsorption studies were performed in a conventional Pyrex vacuum system (*6*). Standard pretreatment and reduction procedures were applied to each sample prior to adsorption as discussed previously (*6*). Volumetric uptakes were converted to mean crystallite dimensions using appropriate assumptions for adsorbate stoichiometry, crystallite shape, and crystallite accessibility (*6–8*).

Carbon monoxide and oxygen chemisorptions were also measured for comparison purposes. Carbon monoxide coverages were obtained from isotherms collected at 298 K and by means of a 373 K temperature jump. Oxygen uptakes were determined at 298 K by static adsorption isotherms and in some instances by pulse adsorption methods to minimize subsurface oxidation (*4*). It should be mentioned that even though temperature-jump methods were used, CO cracking and/or carbonyl formation did not appear to be significant since the increase in adsorption tempera-

ture from 298 to 373 K caused only a ca. 15% increase in CO adsorption.

X-ray line broadening. X-ray diffraction line broadening analysis was performed employing a Phillips Model XRG 2500 diffractometer with a CuKα source. Average crystallite size was estimated using the Debye–Scherrer equation. The line broadening at half-maximum was corrected for instrumental broadening using Warren's equation (*9*), and the net broadening used to calculate the average crystallite size.

RESULTS AND DISCUSSION

Crystallite Size Measurements by Different Methods

a. Carbon monoxide adsorption. Table 1 provides crystallite size determinations obtained using the above-noted procedures. Both the CO/H and O/H uptake ratios increased with decreasing crystallite size. For the case of carbon monoxide, the CO/H ratio increased from 0.64 to 4.75 as the average crystallite size decreased from 21.4 to 3.5 nm. This result was in general agreement with the work of Dalla Betta (*2*) and Yang and Goodwin (*3*). The former author reported that on a low-dispersion ruthenium powder ($d = 10^3$ nm) the CO/H ratio was 0.63; whereas, for ruthenium crystallites supported on alumina ($d = 1.4$ nm), the CO/H ratio increased to 3.8. A similar result has been found by Yang and Goodwin on zeolite-supported ruthenium catalysts except that a higher CO/H ratio of 4.89 was observed for 0.9-nm crystallites. Since hydrogen is known to have a $H/Ru_{(s)}$ adsorption stoichiometry of one (*5, 8*), the above trends indicate that bridge bonding between CO and Ru is favored on large crystallites while surface carbonyls such as $Ru(CO)_2$, $Ru(CO)_3$, $Ru_3(CO)_{12}$, and $Ru(CO)_5$ may be formed as ruthenium crystallites become smaller (*2, 3, 10*). It is also possible that ruthenium cations isolated on the support or located at the periphery of metal crystallites may adsorb multiple carbon monoxide molecules while being unable to be fully reduced or to supply sufficient electron density to dissociate incoming hydrogen molecules. In the context of this study, it is still unclear how 0.9-nm (*3*), 1.4-nm (*2*), and 3.5-nm crystallites

TABLE 1

Characterization of Ruthenium Crystallite Size by Different Methods

Catalyst	Upper ratios			Average crystallite size		Reference
	CO/H[a]	O/H[b]	O/H[c]	$\bar{d}_{H_2}$, 373 K (nm)	$\bar{d}_{XRD}$ (nm)	
I-0.5% Ru/Al_2O_3	—	—	0.57	2.2	—	This work
I-0.5% Ru/Al_2O_3	4.75	—	—	3.5	—	This work
V-2.1% Ru/Al_2O_3	—	1.45	—	4.5	—	This work
C-4.7% Ru/Al_2O_3	1.75	—	—	7.7	—	This work
0.82% Ru/Al_2O_3	—	0.70	—	8.9	—	4
5% Ru/Al_2O_3	0.52	—	—	9.6	—	2
I-5.0% Ru/Al_2O_3	0.65	0.85	0.54	13.4	15.2	This work
C-4.7% Ru/Al_2O_3 (sintered)	0.64	—	—	21.4	—	This work
Ru powder	0.63	—	—	10^3	—	2

[a] Both CO and H_2 uptakes were measured by the 373 K temperature-jump procedure.

[b] O_2 uptake measured by 298 K isotherms.

[c] O_2 uptake measured by pulse chemisorption at 298 K.

can coordinate an average of 4.89, 3.8, and 4.75 carbon monoxide molecules per surface ruthenium atom, respectively; unless the high CO/H ratios observed are biased by the formation of carbonyls and/or suppressed H_2 uptakes as demonstrated in Part I of this study (*6*).

b. Oxygen adsorption. There have been a number of different reports concerning the surface stoichiometry which occurs during oxygen adsorption onto ruthenium. Some investigators (*4, 11*) favor a stoichiometry of RuO while others (*7, 12–14*) believe that RuO_2 surface species are formed. The results of this work reveal a changing O/H uptake ratio which depends on ruthenium crystallite size, and the measurement method employed (i.e., static adsorption versus pulse adsorption).

Using the static approach at 298 K and a first dose pressure of 30 Torr, an O/H ratio of 1.45 was obtained on crystallites of 4.5 nm, whereas, a ratio of 0.85 was found for 13.4-nm crystallites at similar conditions. An even lower O/H ratio of 0.54 was measured by the pulse technique (see Table 1) on the 13.4-nm crystallites at 298 K. These results indicate that the $O/Ru_{(s)}$ stoichiometry appears to depend on adsorption conditions. It is conceivable that higher O/H ratios are obtained on smaller crystallites using the static adsorption method, since these highly dispersed crystallites are less stable toward bulk oxidation, especially when excessive contacting times and/or higher adsorption pressures are used. Subsurface or even bulk oxides may be formed resulting in increased oxygen uptakes. The work of Taylor (*4*) supports this argument by showing that static oxygen uptakes at 296 K are significantly higher compared to those measured at 195 K over 1.6-nm crystallites. On the other hand, oxygen uptakes determined over sintered samples were essentially the same at 296 and 195 K (*4*). Since literature values for $O/Ru_{(s)}$ stoichiometries and O/H adsorption ratios are typically obtained from samples with different crystallite sizes, the above arguments may explain the discrepancies noted by different workers (*4, 7, 11–14*). It is possible, however, that at least one source for the above-noted discrepancies may result from the suppression of hydrogen adsorption by chlorine adatoms, as noted in Part I of this study (*6*).

c. X-ray line broadening. X-ray diffraction line broadening was also employed for the I-5.0% Ru/Al_2O_3 catalyst specimens previously used for CO, O_2, and H_2 adsorption studies. The measured crystallite size provided by XRD was 15.2 nm and represented an average value obtained from the (110), (102), (002), and (100) reflections of 15.5, 15.0, 15.2, and 15.0 nm, respectively. This average value and that calculated from static hydrogen adsorption data at 373 K (i.e., 13.4 nm) appear to agree well with one another.

Dependence of Hydrogen Chemisorption on Crystallite Size

Hydrogen adsorption isotherms were measured on two supported ruthenium catalysts with different crystallite size over the temperature range from 273 to 373 K. For an I-0.43% Ru/Al_2O_3 (2.6 nm) catalyst, a twofold increase in irreversible hydrogen uptake, from 3.2 to 6.4 μmole/g, was observed as the adsorption temperature was increased from 273 to 373 K, whereas, similar efforts applied to a C-4.7% Ru/Al_2O_3 (13.5 nm) catalyst increased the irreversible hydrogen uptake from 13.2 to 14.8 μmole/g. These results demonstrate that irreversible hydrogen uptakes increase with increasing adsorption temperature, and that this phenomenon is particularly evident over smaller crystallites. The above trends are consistent, in general, with the observations of Zowtiak *et al.* (*15*) who noted a similar effect of hydrogen adsorption on silica- and alumina-supported cobalt catalysts prepared from cobalt nitrate. The results of both of these works suggest that hydrogen chemisorption is more highly activated on supported Group VIII metal catalysts of

low loading and presumably smaller average crystallite size.

Based on the above-noted findings further studies were undertaken to elucidate the crystallite size dependency for the activated chemisorption of hydrogen. Since it has been shown earlier that activated hydrogen adsorption results from the presence of surface chlorine adatoms (*6*), this effort was approached by monitoring the relative effects of chlorine additives on crystallites of different size. Three chlorine-free catalyst precursors were prepared by the vapor decomposition/deposition of $Ru_3(CO)_{12}$ to form V-2.3% Ru/Al_2O_3 (2.8 nm), V-2.2% Ru/Al_2O_3 (8.7 nm), and V-1.8% Ru/SiO_2 (9.4 nm). Samples from each precursor batch were chlorinated by dosing to incipient wetness with an aqueous solution of HCl of appropriate concentration. Ratios of the number of dosed chlorine atoms to the number of surface ruthenium atoms, $Cl_{(d)}/Ru_{(s)}$, ranged from 0.1 to 50.0, 0.1 to 166.0, and 0.1 to 210.0, respectively. After chlorine addition, samples were dried at 353 K for 12 h and stored for subsequent use. Prior to adsorption studies these samples were reduced at 673 K for 12 h following the procedure described earlier (*6*). All chlorine analyses were performed on these catalyst samples following reduction and subsequent chemisorption measurements.

Two performance indices, namely, (i) the percentage of sites activated and (ii) the

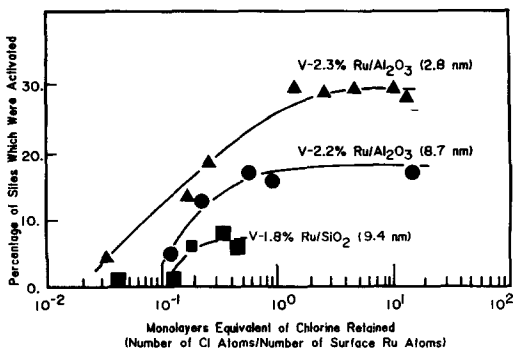

FIG. 1. Percentage of sites activated versus the amount of chlorine retained.

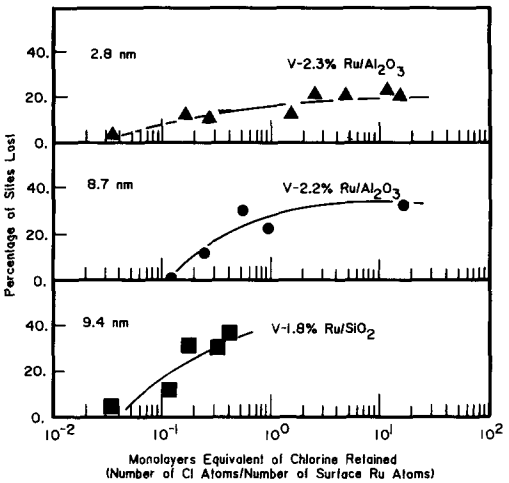

FIG. 2. Percentage of sites lost versus the amount of chlorine retained.

percentage of sites lost, were recorded during hydrogen adsorption studies over these chlorinated specimens. Values of these indices were measured by a 373 K temperature-jump procedure as described earlier. Since activated hydrogen chemisorption was not observed over chlorine-free specimens, the difference in hydrogen uptake before and after the temperature jump was taken, by definition, to indicate the number of sites which became activated by chlorine. Differences in irreversible hydrogen uptakes at 373 K, between chlorinated catalysts and unchlorinated precursors, were used to represent the number of hydrogen adsorption sites which were blocked by chlorine adatoms. It should be noted that this loss of adsorption sites was not caused by catalyst sintering during treatments involving chlorine addition. Indeed, control studies showed that essentially all adsorption sites could be recovered after catalysts were dosed to incipient wetness with chlorine-free distilled water.

Figures 1 to 5 summarize results obtained from studies of the effects of chlorine versus crystallite size. The ratio of the number of chlorine atoms retained by the catalyst after reduction to the number of surface ruthenium atoms before the addition of chlorine ($Cl_{(r)}/Ru_{(s)}$) is denoted as the mono-

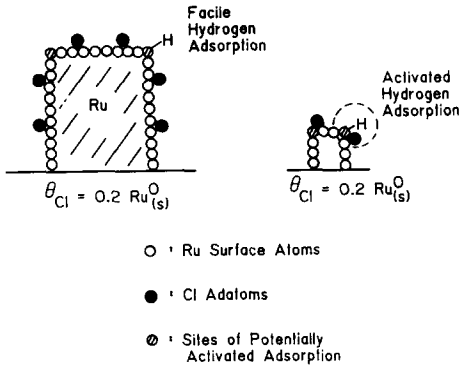

FIG. 3. Simplified model for interactions between chlorine adatoms and surface ruthenium atoms versus crystallite size.

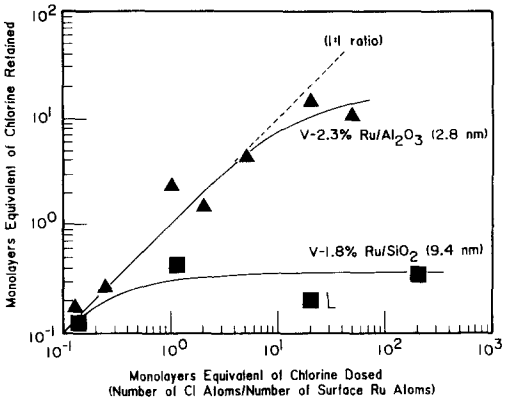

FIG. 5. Monolayers equivalent of chlorine retained versus monolayers equivalent of chlorine dosed.

layers equivalent of chlorine retained. This quantity was determined by means of bulk analyses before and after chlorine dosage (Galbraith).

Figure 1 shows that for all three catalysts examined, the percentage of sites which become activated by the addition of chlorine increases initially with the $Cl_{(r)}/Ru_{(s)}$ ratio. This trend ceases when the surface becomes "saturated" with chlorine. Comparison of the two Ru/Al_2O_3 catalysts of different crystallite size, i.e., V-2.3% Ru/Al_2O_3 (2.8 nm) and V-2.2% Ru/Al_2O_3 (8.7 nm), shows that a larger fraction of sites (ca. 30%) can become activated following chlorine addition compared to the results obtained over 8.7-nm crystallites (ca. 17%).

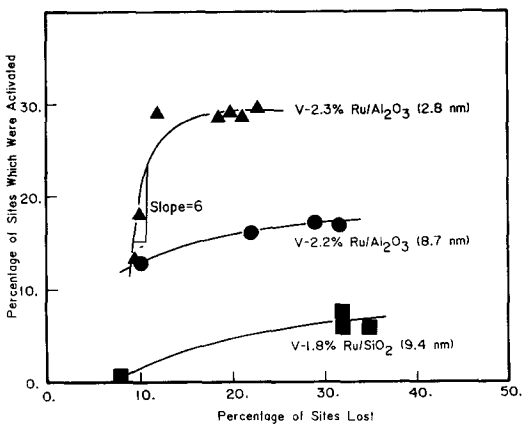

FIG. 4. Percentage of sites activated versus percentage of sites lost.

Figure 2 shows the loss of hydrogen chemisorption sites versus the amount of chlorine retained. Although all samples exhibit the same trend, a greater fraction of sites are removed from larger crystallites following chlorine addition, suggesting that chlorine adatoms prefer high coordination sites. The fact that over small crystallites more sites become activated while less sites are lost indicates that low coordination sites, available in greater proportions on small crystallites, are mainly responsible for activated chemisorption behavior. Chlorine adsorption therefore causes a reduction in the electron density at associated/adjacent low-coordination sites which results in an increased energy barrier for electron donation to incoming hydrogen molecules. This reduced electron density then accounts for the observed increase in the activation energy for dissociative hydrogen adsorption (*6*).

A number of factors may be responsible for the higher propensity of small crystallites to exhibit chlorine-induced activated chemisorption. First, small crystallites contain fewer ruthenium atoms and are therefore expected to be more perturbed by an electronegative adsorbate in a fashion commensurate with the surface-to-volume ratio (i.e., dispersion) of the crystallite. This effect will be further enhanced since low-coordination sites, which are found in greater

proportions on small crystallites, are apparently responsible for activated hydrogen adsorption. Second, if the previously discussed electronic perturbation by adatoms has a short-range effect, then small crystallites are expected to provide higher proportions of potentially activated low-coordination metal sites *in close proximity* to high-coordination sites suitable for chlorine adsorption. The above reasoning leads to a two-site model illustrated in Fig. 3 which requires chlorine adsorption sites adjacent to, or in close proximity with, low-coordination surface ruthenium atoms.

In formulating the model shown in Fig. 3, a number of alternate explanations had to be discarded. Among those considered were (i) the effects produced by adsorption/activation in the vicinity of the metal–support interface and (ii) the adsorption behavior produced as a result of direct bonding between hydrogen and chlorine adatoms. In the first instance, it is expected that if activated hydrogen adsorption sites and chlorine adsorption sites involve the interfacial perimeter of the crystallite, then both the number of sites activated *and* the number of sites poisoned will increase with increasing dispersion—due to the fact that smaller crystallites have larger relative proportions of interfacial sites. In the second case, it is suspected that if activated hydrogen adsorption sites involve direct bonding of hydrogen to chlorine, then the number of sites activated will increase with increasing crystallite size—as a result of the fact that larger crystallites retain more chlorine. Since the aforementioned trends were not observed, these alternate models were discounted.

Further verification of the model shown in Fig. 3 can be obtained from Fig. 4, where the percentage of activated adsorption sites is compared to the number of sites lost due to chlorine adsorption. In this instance, it can be seen that at a fixed level of chlorine poisoning, the percentage of sites which become activated is generally higher on smaller crystallites. Moreover, at low chlorine levels on small crystallites, addition of each chlorine adatom can produce up to six activated hydrogen adsorption sites. This trend, however, is not as significant for larger crystallites indicating that fundamental differences in adsorption behavior are encountered as crystallite size is decreased in the presence of chlorine. Other evidence for a site-dependent activation mechanism is provided by the observation that the number of activated sites produced by chlorine addition becomes constant even though the number of chlorine adatoms continues to increase (see Fig. 4).

Effect of Support

Also evidenced by Figs. 1, 2, and 4 is the fact that silica-supported ruthenium catalysts do not provide as many activated adsorption sites as alumina-supported ruthenium catalysts when crystallites of similar size are considered (viz., 8.7 versus 9.4 nm). It appears that more sites are blocked by chlorine addition to silica-supported crystallites than are blocked by chlorine addition to alumina-supported crystallites. For example, over V-1.8% Ru/SiO_2 (9.4 nm) catalysts only 7% of the total number of adsorption sites, measured before chlorine addition, become activated after blockage of 35% of the adsorption sites, whereas, for V-2.2% Ru/Al_2O_3 (8.7 nm) catalysts 17% of the total number of adsorption sites become activated after blockage of 30% of the adsorption sites. These observations suggest that the catalyst support may participate in the chlorine-induced activated chemisorption of hydrogen, possibly by alteration of the crystallite shape and thus the ratio of low-coordination to high-coordination adsorption sites.

Zowtiak *et al.* (*15*) reported that H_2 adsorption was more highly activated on alumina-supported cobalt catalysts relative to silica-supported specimens. They attributed this behavior to stronger metal–support interactions. However, it should be noted that incomplete reduction of their

alumina-supported catalysts as compared to their silica-supported catalysts could also provide an explanation for this behavior since residual oxygen and nitrogen remaining after reduction/decomposition of cobalt nitrate precursors may have had similar effects to that of chlorine. Indeed, oxygen and nitrogen have electronegativities of 3.50 and 3.05 on the Pauling scale, respectively, whereas chlorine has a value of 3.15 (*16*). Furthermore, since specimens with different supports and differing degrees of reduction were compared, it is likely that crystallites of different size and shape have been compared.

An examination of the amount of chlorine retained versus the amount of chlorine dosed on catalysts used in this study (Fig. 5) shows that the saturation uptake of chlorine is much less on silica-supported catalysts than on alumina-supported catalysts. These results demonstrate the different affinities which SiO_2 and Al_2O_3 possess toward chlorine accommodation. However, as discussed previously, chlorine adsorbed on the support has little effect on the modification of chemisorption properties. Changes in the number of activated chemisorption sites and chlorine blocked sites all occurred at chlorine dosage levels below one monolayer (Figs. 1 and 2). Therefore, a long-range modification or inductive effect through a support-mediated charge transfer mechanism, such as that proposed by Aika *et al.* (*17*), was not evident. Most likely, different structural morphologies of ruthenium crystallites when supported on SiO_2 or Al_2O_3 change the ratio of low-coordination to high-coordination sites and account for the apparent support effect. If this is the case, then it is possible that deliberate addition of chlorine may provide a sensitive probe for determining details concerning crystallite shape and surface texture, whereas, traditional hydrogen chemisorption studies require assumption of the crystallite shape.

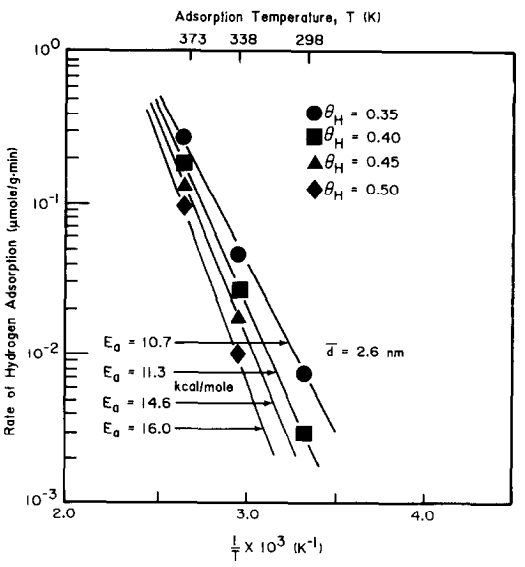

FIG. 6. Arrhenius plot of hydrogen chemisorption on an I-0.43% Ru/Al_2O_3 catalyst. θ_H is the hydrogen surface coverage, E_a is the apparent activation energy for hydrogen chemisorption in kcal/mole. $Cl_{(r)}/Ru_{(s)}$ = 10.75.

Activation Energies for Adsorption

Apparent activation energies for hydrogen chemisorption were measured over catalysts with different average crystallite sizes using the methods and procedures described earlier (*6*). These catalysts were I-0.43% Ru/Al_2O_3 (2.6 nm), I-0.48% Ru/SiO_2 (6.5 nm), and C-4.7% Ru/Al_2O_3 (13.5 nm) with $Cl_{(r)}/Ru_{(s)}$ ratios of 10.75, 3.62, and 2.08, respectively, based on bulk chlorine analyses. Since chlorine levels retained by these catalysts following impregnation all exceeded one monolayer, the chlorine adsorption sites on the surfaces of the ruthenium crystallites are most likely fully populated by chlorine.

The Arrhenius plot for the I-0.43% Ru/Al_2O_3 (2.6 nm) sample is shown in Fig. 6 while the apparent activation energies measured over all three samples are tabulated in Table 2. As demonstrated in Fig. 6, there is a general trend toward increasing activation energy with increasing coverage, indicating that either surface diffusion and rearrangement of adsorbed hydrogen is involved or more likely that sites with higher

TABLE 2

Apparent Activation Energies for Hydrogen Chemisorption on Catalysts with Varying Crystallite Size

Catalyst	Average crystallite[a] size (nm)	Surface chlorine level ($Cl_{(r)}/Ru_{(s)}$)	Apparent[b] activation energy (E_a, kcal/mole)
C-4.7% Ru/Al_2O_3	13.5	Saturated[c]	4–5
I-0.47% Ru/SiO_2	6.5	Saturated[c]	9–10
I-0.43% Ru/Al_2O_3	2.6	Saturated[c]	15–16

[a] Determined by hydrogen chemisorption at 373 K. Uptake has not been corrected for sites poisoned by chlorine.

[b] Activation energies measured at half saturation coverage of hydrogen.

[c] Refers to complete population of that fraction of the surface ruthenium sites which can accommodate chlorine adatoms.

activation energy are being encountered as coverage increases. Indeed, it is conceivable that a range of adsorption activation energies are encountered over these polycrystalline catalyst samples and that adsorption proceeds most readily on sites of low activation energy so that rates measured at higher coverages are representative of adsorption on sites of higher activation energy. Furthermore, it can be reasoned, based on preceding discussions, that the distributions of activation energies may depend on the ratio of low-coordination to high-coordination sites which is governed by the size and shape of the crystallite. Table 2 shows that apparent activation energies for adsorption at half saturation coverage of hydrogen range between 4–5, 9–10, and 15–16 kcal/mole on crystallites with average sizes of 13.5, 6.5, and 2.6 nm, respectively. These results confirm the fact that increasingly more activated adsorption is encountered with decreasing crystallite size.

Correlation of Activated Chemisorption with Crystallite Size

To more quantitatively address the effects of crystallite size on activated hydrogen chemisorption, a correlation has been made between the percent increase in irreversible hydrogen uptake after a "temperature jump" versus average crystallite size. Values of these temperature-jump measurements are presented in Table 3. The catalysts used in this correlation were all prepared by incipient wetness using $RuCl_3$. These results (Fig. 7) may thus be representative of other ruthenium catalysts in which a chlorine containing ruthenium salt is used during the impregnation process. Since this preparation method generates a high concentration of chlorine during the decomposition of $RuCl_3$, it is believed that most of the available chlorine adsorption sites on the surface of these ruthenium crystallites are fully populated by chlorine as suggested by the observations of the previous section and subsequent discussions. Therefore, the question of chlorine concentration is included in the correlation through the inherent capacity of a particular size crystallite to accommodate surface chlorine. Efforts similar to these have been reported by Don *et al.* (*18*) following preparation of unsupported ruthenium catalysts from $RuCl_3$, al-

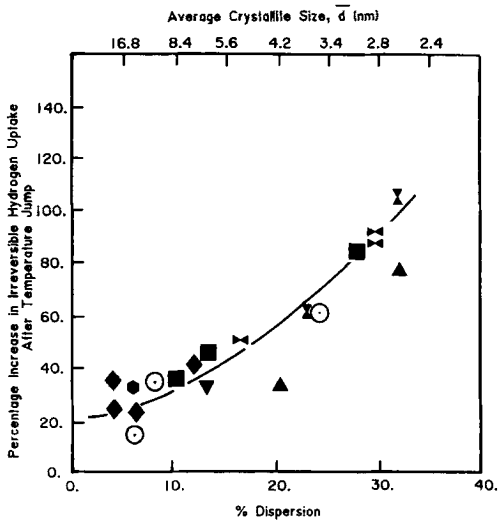

FIG. 7. Percentage increase in irreversible hydrogen uptake after a temperature-jump versus percentage dispersion. Results obtained from a variety of Ru/Al_2O_3 and Ru/SiO_2 specimens prepared by incipient wetness impregnation using $RuCl_3$. Circled data points were obtained from chlorine-free specimens subsequently dosed with chlorine; see text for calculation procedure.

TABLE 3

Results of Temperature-Jump Experiments on Supported Ruthenium Catalysts of Various Crystallite Size

Catalyst	Symbol	$\bar{d}$ (nm)[a]	% Dispersion	% Increase in irreversible hydrogen uptake after temperature jump
a. I-0.43% Ru/Al_2O_3	▲	2.6	32	77
b. I-0.50% Ru/Al_2O_3 batch (I)	⧗	2.6	32	105
c. I-0.50% Ru/Al_2O_3 batch (II)	⋈	2.9	29	89
d. Same as c[b]	⋈	2.9	29	91
e. I-2.0% Ru/Al_2O_3	■	3.0	28	84
f. Same as b[b]	⧗	3.5	24	60
g. Same as a[b]	▲	4.2	20	32
h. Same as c[b]	⋈	5.1	16	51
i. 0.48% Ru/SiO_2	▼	6.5	13	34
j. Same as e[b]	■	6.6	13	45
k. C-4.7% Ru/Al_2O_3	◆	7.7	12	42
l. Same as e[b]	■	8.8	10	35
m. I-5.0% Ru/Al_2O_3	●	13.4	6	30
n. Same as k[b]	◆	13.5	6	23
o. Same as k[b]	◆	21.4	4	35
p. Same as k[b]	◆	22.0	4	24

[a] Determined by hydrogen chemisorption at 373 K. Uptake has not been corrected for sites poisoned by chlorine.

[b] Larger crystallites obtained by controlled sintering.

though, the formation and measurement of activated adsorption sites were not considered.

It can be seen from Fig. 7 that a smooth trend exists between the density of activated sites and crystallite size. This trend may have significant implications toward the measurement of ruthenium surface areas on highly dispersed catalysts prepared from $RuCl_3$. A greater than twofold underestimation of the ruthenium surface area may result from hydrogen measurements at 298 K. Agreement with the above correlation is found in the work of Zagli and Falconer (*19*). In their case, a 108% increase in the irreversible hydrogen uptake was observed for a 37% dispersed Ru/SiO_2 catalyst prepared from $RuCl_3$ as the adsorption temperature was increased from 298 to 363 K.

It should be mentioned that the crystallite sizes used in the above correlation were calculated from irreversible hydrogen uptakes after a 5.5-h, 373 K temperature jump. These uptakes, obtained on catalysts prepared by incipient wetness impregnation using $RuCl_3$, do not take into account the number of sites lost by strongly bound chlorine. Therefore, the calculated average crystallite size provides values which are larger than their "true" size. With this in mind, a back calculation was made using data obtained from catalysts prepared by vapor decomposition of $Ru_3(CO)_{12}$ in the absence of chlorine to test the validity of the above correlation. In this calculation, the "true" crystallite size of the catalyst precursor prepared from the vapor decomposition/deposition method was first obtained, adjusted for the percentage of sites blocked by chlorine (Fig. 2), and an "effective new crystallite size" calculated as if no sites had been blocked by chlorine. This "new" crystallite size corresponds to the

size that one would calculate from adsorption data at 373 K should the catalyst be exposed to copious amounts of chlorine or prepared by incipient wetness impregnation using $RuCl_3$. The percent increase in irreversible hydrogen uptake after the temperature jump for the chlorine-doped catalyst, made from a chlorine-free precursor, is then calculated on a basis which does not include the number of sites blocked by chlorine. Data obtained from chlorine-free catalysts can, in this way, be compared with adsorption results obtained from catalysts prepared using $RuCl_3$.

For demonstration purposes, data obtained following chlorine addition to a V-2.3% Ru/Al_2O_3 catalyst are used in the above-noted fashion to compare hydrogen adsorption on this catalyst to one prepared from $RuCl_3$.

V-2.3% Ru/Al_2O_3:

Actual average crystallite size:

$$(d)_t = 2.8 \text{ nm};$$

percentage of sites lost after extensive chlorine addition:

$$(P)_L = 20\%;$$

percentage of sites activated after extensive chlorine addition:

$$(P)_A = 30\%;$$

new average crystallite size:

$$(d)_n = \frac{(d)_t \times (\text{uptake})_t}{(\text{uptake})_t \times (1 - (p)_L)} = 3.5 \text{ nm}.$$

The total irreversible hydrogen uptake without chlorine addition, $(\text{uptake})_t$, corresponds to the sum of (i) sites which are measured by hydrogen chemisorption at 298 K after 24 h, (ii) sites which become activated by adsorbed chlorine, and (iii) sites which are blocked by adsorbed chlorine.

The percentages of each of these three types of sites are denoted as $(P)_R$, $(P)_A$, and $(P)_L$, respectively. Therefore,

$$(P)_R + (P)_A + (P)_L = 100\%.$$

The percent increase in irreversible uptake after the temperature jump, by definition, equals

$$\frac{(p)_A}{(p)_R} = \frac{30\%}{(100\% - 30\% - 20\%)} = 60\%.$$

This calculated data point (i.e., 60% increase in irreversible uptake after a "temperature jump" for a 3.5-nm crystallite) correlates well with the trend shown in Fig. 7. Similar calculations were also made for V-2.2% Ru/Al_2O_3 and V-1.8% Ru/SiO_2 catalysts. The results are shown in Fig. 7 as open circles. These data once more suggest that catalysts prepared using incipient wetness impregnation of $RuCl_3$ are similar to those prepared in a chlorine-free environment and subsequently saturated by chlorine.

It is interesting to note that if similar adsorption calculations are performed for the V-2.3% Ru/Al_2O_3 (2.8 nm) catalyst, with no allowance made for activated adsorption or site blockage by chlorine, a crystallite size of 5.6 nm is obtained. This result demonstrates that chlorine blockage and activated adsorption can introduce significant errors in surface area measurements. Furthermore, it is expected that this effect may become more significant as crystallite size is reduced.

SUMMARY

The effect of chlorine adatoms on the chemisorption properties of alumina-supported ruthenium crystallites has been investigated over a range of crystallite size. A relatively short-ranged electronic modification attributable to chlorine was observed. Electronegative chlorine adatoms appear to preferentially adsorb on high-coordination surface sites and inhibit electron donation to incoming hydrogen molecules at adjacent lower-coordination sites. As a consequence, hydrogen chemisorption on these low-coordination sites becomes activated. More importantly, this effect is observed to increase as the average crystallite size is reduced. The apparent activation energies

for hydrogen chemisorption, measured at approximately half saturation coverage on ruthenium crystallites prepared from $RuCl_3$, were 4–5, 9–10, and 15–16 kcal/mole on crystallites of 13.5, 6.5, and 2.6 nm diameter, respectively.

A good correlation exists between the density of highly activated sites and crystallite size. This correlation suggests that for ruthenium surfaces containing chlorine adatoms, a greater than twofold underestimation of surface ruthenium atoms may result from hydrogen chemisorption measurements at 298 K.

Comparison of data collected over silica- and alumina-supported ruthenium catalysts suggest that chlorine has different effects on these two catalysts even though crystallites of similar dispersion were compared. This indirect support effect may be attributed to the alteration of crystalline shape and thus the ratio of low-coordination to high coordination sites. It is possible that deliberate addition of chlorine may provide a sensitive probe for discriminating differences in crystallite shape and surface texture.

ACKNOWLEDGMENTS

Support for this work is acknowledged from the Department of Energy (DEAC 2283PC6044) and the Auburn University Engineering Experiment Station.

REFERENCES

1. Lam, Y. L., and Sinfelt, J. H., *J. Catal.* **42,** 319 (1976).
2. Dalla Betta, R. A., *J. Phys. Chem.* **79**(23), 2519 (1975).
3. Yang, C. H., and Goodwin, J. G., Jr., *React. Kinet. Catal. Lett.* **20**(1–2), 13 (1982).
4. Taylor, K. C., *J. Catal.* **38,** 299 (1975).
5. Sayari, A., Wang, H. T., and Goodwin, J. G., Jr., *J. Catal.* **93,** 368 (1985).
6. Lu, K., and Tatarchuk, B. J., *J. Catal.* **106,** 166 (1987).
7. Goodwin, J. G., Jr., *J. Catal.* **68,** 227 (1981).
8. Dalla Betta, R. A., *J. Catal.* **34,** 57 (1974).
9. Klug, H. P., and Alexander, L. E., "X-Ray Diffraction Procedure," 2nd ed. Wiley, New York, 1974.
10. Kobayashi, M., and Shirasaki, J., *J. Catal.* **28,** 289 (1973).
11. Buyanova, N. E., Karnoukhov, A. P., Koroleva, N. G., Ratner, I. D., and Chernyavskaya, O. N., *Kinet. Katal.* **13,** 1533 (1972).
12. Gay, I. D., *J. Catal.* **80,** 231 (1983).
13. Kubicka, H., *React. Kinet. Catal. Lett.* **5,** 223 (1974).
14. Corro, G., and Gomez, R., *React. Kinet. Catal. Lett.* **12,** 145 (1979).
15. Zowtiak, J. M., Weatherbee, G. D., and Bartholomew, C. H., *J. Catal.* **82,** 230 (1983).
16. Dean, A. J., Ed. "Lange's Handbook of Chemistry" 12th ed. McGraw-Hill, New York, 1979.
17. Aika, K., Hori, H., and Ozaki, A., *J. Catal.* **27,** 424 (1972).
18. Don, J. A., Pijpers, A. P., and Scholten, J. J. F., *J. Catal.* **80,** 296 (1983).
19. Zagli, E., and Falconer, J. F., *J. Catal.* **69,** 1 (1981).